Environmental Science & Technology

pubs.acs.org/est

Article

Contribution of Microorganisms with the Clade II Nitrous Oxide Reductase to Suppression of Surface Emissions of Nitrous Oxide

Kristopher A. Hunt,* Alex V. Carr, Anne E. Otwell, Jacob J. Valenzuela, Kathleen S. Walker, Emma R. Dixon, Lauren M. Lui, Torben N. Nielsen, Samuel Bowman, Frederick von Netzer, Ji-Won Moon, Christopher W. Schadt, Miguel Rodriguez Jr, Kenneth Lowe, Dominique Joyner, Katherine J. Davis, Xiaoqin Wu, Romy Chakraborty, Matthew W. Fields, Jizhong Zhou, Terry C. Hazen, Adam P. Arkin, Scott D. Wankel, Nitin S. Baliga, and David A. Stahl

Cite This: *Environ. Sci. Technol.* 2024, 58, 7056−7065

Read Online

ACCESS | Metrics & More | Article Recommendations | Supporting Information

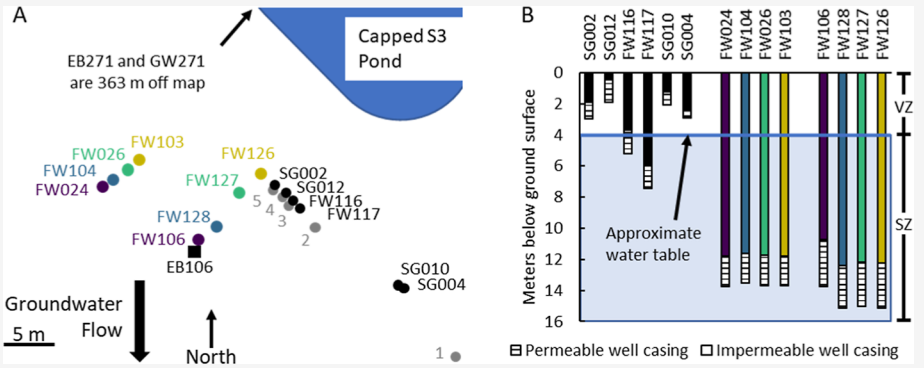

ABSTRACT: The sources and sinks of nitrous oxide, as control emissions to the atmosphere, are generally poorly constrained for most environmental systems. Initial depth-resolved analysis of nitrous oxide flux from observation wells and the proximal surface within a nitrate contaminated aquifer system revealed high subsurface production but little escape from the surface. To better understand the environmental controls of production and emission at this site, we used a combination of isotopic, geochemical, and molecular analyses to show that chemodenitrification and bacterial denitrification are major sources of nitrous oxide in this subsurface, where low DO, low pH, and high nitrate are correlated with significant nitrous oxide production. Depth-resolved metagenomes showed that consumption of nitrous oxide near the surface was correlated with an enrichment of Clade II nitrous oxide reducers, consistent with a growing appreciation of their importance in controlling release of nitrous oxide to the atmosphere. Our work also provides evidence for the reduction of nitrous oxide at a pH of 4, well below the generally accepted limit of pH 5.

KEYWORDS: *nitrous oxide, denitrification, chemodenitrification, nosZ, isotopic fractionation, flux, pH*

INTRODUCTION

Increasing nitrous oxide in the atmosphere, an ozone-destructive and potent greenhouse gas with an atmospheric half-life of more than 100 years,[1] is associated primarily with its emission from low oxygen aquatic systems, wastewater treatment, and systems impacted by changing land use and agriculture. Produced by both biotic and abiotic processes, the only known sink for nitrous oxide below the stratosphere is the microbial reduction to N_2 by the nitrous oxide reductase (NosZ) enzyme. Although nitrous oxide is a thermodynamically more favorable electron acceptor (E^0 = 1.77 V) than oxygen (E^0 = 0.815 V), competition experiments with characterized facultative anaerobes have shown that nitrous oxide reduction is not always the preferred electron acceptor over a wide range of oxygen concentrations.[2−4] This could reflect the stoichiometric differences in energy yield for the alternative substrates since oxygen has a higher energy yield than nitrous oxide on a mole of oxidant basis and may be the more relevant limiting substrate in many environments. Regardless of mechanism, what would appear to be a highly favorable electron acceptor even in the presence of oxygen is lost to the atmosphere from many environments, including soils (0.0006 ± 0.0023 μmol m^{-2} s^{-1} [mean ± standard

Received: September 25, 2023
Revised: March 29, 2024
Accepted: April 1, 2024
Published: April 12, 2024

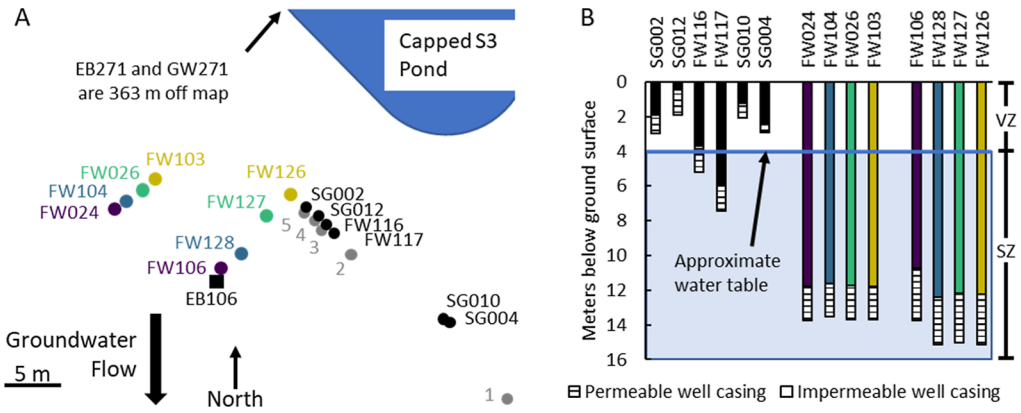

Figure 1. (A) Schematic of the field site showing the location of the contamination source (capped S3 pond) and sampling locations. Wells that were sampled for isotopic analysis and chemistry are represented by colored circles. Wells monitored for nitrous oxide flux are shown as black circles. Surface positions for flux measurements are marked with gray circles. The location of sediment core EB106 is marked with a black square. (B) Profile of well screen depths (striped region) used for groundwater sampling. The approximate location of the groundwater table is designated with a horizontal blue line, and the VZ and SZ are annotated to the right of the figure.

deviation][5−10]), marine systems (0.0019 ± 0.0035 μmol m^{-2} s^{-1}[11−16]), and freshwater systems (0.0029 ± 0.0068 μmol m^{-2} s^{-1}[17]). Since it is primarily the balance between production and microbial consumption that determines the emission to the atmosphere, improved predictive modeling of nitrous oxide emissions will depend on integrated studies designed to resolve the spatial and temporal distribution of its sources and sinks and better constrain the biotic and abiotic variables influencing those processes.

Although terrestrial nitrous oxide consumption is recognized to be solely an enzymatic process, both biotic (denitrification, codenitrification, nitrification, nitrifier-denitrification) and abiotic (chemodenitrification) processes control production. Apart from the need to resolve those alternative sources of production, environmental variables influencing consumption by the activities of organisms expressing the Clade I (a.k.a., typical) or Clade II (a.k.a., atypical) NosZ variant may have a significant impact on emissions of nitrous oxide.[18−20] This is suggested by reports of the differential distribution of these variants in diverse ecosystems, including soils and marine oxygen minimum zones, and a few reports of differences in uptake kinetics and sensitivity to oxygen.[21−24] However, there remains a limited understanding of physiological differences and the environmental variables controlling the distribution and activity of the two variants. This information is essential for improved modeling of the flux of this environmentally active gas to the atmosphere, as well as for developing management tools for abatement.[22]

Here, we present the use of combined activity, molecular, geochemical, gas flux, and isotopic measurements to resolve the sources and sinks of nitrous oxide in a heavily nitrate contaminated low pH groundwater system on the Oak Ridge National Laboratory (ORNL) Reservation.[25] We used the isotopic composition of nitrogen species to qualitatively demonstrate that both biotic and abiotic processes contributed to significant production of nitrous oxide,[26] with biotic production correlated with high numbers of*Rhodanobacter* species.[27−29] In turn, isotopic analyses of nitrous oxide consumption from observation wells, showed active biological reduction at pH values as low as 4, well below values generally thought inhibitory for reduction and only previously observed in a *Rhodanobacter* enriched reactor community.[30] An associated depth-resolved genomic characterization of *nosZ* implicated the Clade II variant in the suppression of surface emissions. Thus, at this site, organisms expressing the Clade II NosZ appear to be the major contributor to the consumption of nitrous oxide, functioning to largely suppress surface emissions of this potent greenhouse gas.[23,24]

MATERIALS AND METHODS

Field Site. The observation wells characterized in this study are located at the Field Research Center (FRC) on the Oak Ridge National Laboratory (ORNL) Reservation and hydraulically down-gradient of the capped contaminant source, previously the S3 disposal ponds at the Y12 site. Leaching of materials disposed in the ponds from radionuclide processing have contributed to a low pH (3−6.5), high nitrate (>1 M) groundwater contaminated by organics, radionuclides, and heavy metals.[31] Most contamination is distributed in the deeper saturated and variably saturated zones (SZs), with less and more variable contamination in the vadose zone (VZ), the region of sediment below the ground surface and above the variably SZ.[32]

Quantification of Nitrous Oxide Flux. Nitrous oxide and carbon dioxide fluxes from multiple well-heads were quantified using a Picarro gas analyzer (G2508), recirculating pump (A0702), Eosense multiplexer (eosMX), and Eosense flux chambers (eosAC) with 30 m connections between the chambers and the multiplexer unit. Flux chambers were mounted on 6 wells located in an area immediately hydraulically down-gradient of the capped S3 disposal ponds (Figure 1). Flux values were determined by averaging the slope of ppm vs time from a 60 s window over data collected from 2 to 5 min after purging the connections. The complete analysis and data are available in the Supporting Information at 10.6084/m9.figshare.24196218. The limit of flux detection for this system was approximately 10^{-4} and 10^{-2} μmol m^{-2} s^{-1} for nitrous oxide and carbon dioxide, respectively.[33] Flux from each location was normalized to the surface area of the flux chamber for surface measurements or the cross-sectional area of the well casing for well measurements (Table S1).

Assays for Biotic and Abiotic Nitrous Oxide Production Activity in the Subsurface. Groundwater biomass collected on filters was used for the acetylene block characterization. Approximately 2 L of groundwater was collected on a 0.22 μm PES membrane filter (Sterlitech) by

https://doi.org/10.1021/acs.est.3c07972
Environ. Sci. Technol. 2024, 58, 7056−7065

vacuum filtration and used to inoculate 160 mL serum bottles containing 50 mL of filtered groundwater with and without nutrient amendment, and with and without acetylene. Each serum bottle received 1/8 segment of the filter, allowing for duplicate incubations. Nitrate and/or organic carbon were amended via 2.5 mL of a 100 mM sodium nitrate solution or a solution containing 100 mM sodium lactate, sodium acetate, monosodium glutamate, and sodium benzoate. The final concentration of nitrate and carbon added was 4.5 mM each, but this does not account for any carbon or nitrogen present in the original sample. Acetylene was added to the headspace to a final concentration of 1% from a 10% acetylene stock in dinitrogen, and the bottles were incubated in the dark at ambient temperature (22 °C). Nitrous oxide accumulation in the headspace was quantified by GC-ECD over a four-day period, collecting gas samples in 12 mL exetainers by 2.5 mL syringe transfer on day 0, 1 mL on day 2, and 0.5 mL on day 4.

Analysis of Nitrate, Nitrite, and Nitrous Oxide Isotopic Composition. Environmental samples for nitrogen and oxygen isotopic characterization were collected from eight wells on October 2, 17, 30, and November 13, 2019 (Figure 1). Samples for nitrous oxide analysis were collected by pumping approximately 100 g of unfiltered groundwater directly into 1 L multilayer foil sampling bags (Restek 22950) to minimize off-gassing. Each bag contained 0.5 mL of 10 M NaOH, to achieve a pH of at least 12 for sample preservation before shipping to the Woods Hole Oceanographic Institution (WHOI) for analysis. All nitrous oxide sampling materials were flushed with dinitrogen gas (Airgas, Radnor, PA) before sample collection to minimize atmospheric contamination. Groundwater for nitrate and nitrite analysis was filtered (0.2 μm PES) and stored in 20 mL Nalgene scintillation vials (ThermoFisher 2003-9050) with minimal headspace before shipping to WHOI for analysis. Water samples for analysis of water δ^2H & δ^{18}O were filtered through 0.2 μm PES syringe filters and stored without a headspace in 2 mL glass GC vials (ThermoFisher C4010-1W) sealed with septa screw caps (ThermoFisher C4010-40A) before shipping to the University of California at Davis for analysis by Off-Axis Integrated Cavity Output Spectroscopy (Off-Axis ICOS). All samples were stored at 4 °C before shipping.

Nitrate stable N and O isotope composition was determined using the denitrifier method, wherein nitrate was quantitatively converted to nitrous oxide by a cultured denitrifying bacteria lacking nitrous oxide reductase.[34,35] Approximately 20−40 nmol of sample nitrate was used to produce nitrous oxide, which was purified and cryogenically trapped using a customized purge-and-trap under a continuous flow of helium before introduction to an Isoprime100 isotope ratio mass spectrometer (IRMS). Nitrate isotope reference materials (USGS 32, USGS 34, and USGS 35) were analyzed periodically to correct any size or drift and to normalize sample isotope composition. Typical reproducibility for δ^{15}N was ±0.3‰ and for δ^{18}O is ±0.4‰. Concentrations of nitrate (working range of 0.5−800 mg/L) were determined on a Dionex ICS-2100 (ThermoFisher Scientific, USA) equipped with an autosampler (Dionex AS40) and an Dionex IonPac AS11-HC column (4 × 250 mm) at room temperature with a KOH effluent gradient of 0−60 mM at 1.0 mL/min. The nitrate concentrations at this site were more than 700-fold higher than accompanying nitrite concentrations; therefore, the impact of nitrite on the analysis of nitrate would be less than the error of the measurement.

Nitrite stable N and O isotope composition was determined after conversion to nitrous oxide in acetic-acid buffered sodium azide,[36] followed by analysis using the same purge-and-trap system described above. Isotopic ratios are reported in reference to calibrated values of internal lab nitrite standards (WILIS 10, WILIS 11, and WILIS 20). Typical reproducibility for δ^{15}N and δ^{18}O is ±0.2 and ±0.3‰, respectively.

Nitrous oxide isotope analyses were conducted as follows. A 0.2 to 2 mL subsample of the headspace from the multilayer foil sampling bags was injected into a 25 mL serum bottle previously purged with ultrahigh purity helium. Subsamples of this primary dilution were injected into evacuated 20 mL autosampler vials for analysis on the purge-and-trap system. Repeat analyses were conducted to account for large variations in the nitrous oxide concentrations of field samples. Isotope ratios (δ^{15}N and δ^{18}O) were normalized by regular comparison to analyses of USGS 51 and USGS 52, which have similar δ^{15}N and δ^{18}O but differing site preference (i.e., the difference between the position specific δ^{15}N composition in the central alpha versus outer beta position in the nitrous oxide molecule), using a semiautomated aliquot system on the purge-and-trap. A range of injection volumes of nitrous oxide isotopic analyses from a reference tank was used to correct for any injection volume linearity effects. Typical reproducibility for δ^{15}N and δ^{18}O was ±0.3 and ±0.4‰, respectively, and ±1.0‰ for site preference. Normalized isotopic signatures were calculated as described in Yu et al. 2020,[26] equations can also be found in the Supporting Information.

Depth Resolved Metagenomic Analysis of Denitrification Gene Distribution in Sediment Cores. DNA recovered from sediment samples was sequenced by using the Illumina platform for metagenome assembly. DNA extraction, sequencing, read quality control, and assembly are described in Lui et al. 2024.[37] Briefly, DNA was extracted using the Qiagen PowerMax soil kit with some modifications as described by Lui et al. 2024 and Wu et al. 2023 and prepped with the Illumina Nextera Flex kit (now called the Illumina DNA Prep kit).[37,38] Reads were deposited in NCBI's Sequence Read Archive in BioProject PRJNA1001011 under accession numbers SAMN36786281-SAMN36786357. Illumina reads were quality filtered and trimmed using BBTools 38.86 and assembled with SPAdes Version 3.15.4.[39−41]

A table of metagenome parameters and relevant sample information is included in the Supporting Information (Table S3). Samples were coassembled if they were sample replicates from the same groundwater or sediment sample. Co-assemblies are outlined in Table 1 of Lui et al. 2024.[37] Genes were called using Prodigal Version 2.6.3 with parameters "-c-n-p meta".[42] Gene annotation was accomplished using eggNOG-mapper version 2.1.7 with parameters "-m diamond-query_cover 50-subject_cover 50".[43] Individual genes (e.g., nosZ) were extracted using a textual search on the annotation output. Quality-filtered and trimmed reads were mapped to contigs to obtain coverage values using BWA version 0.7.17-r1188.[44] We used the BWA-MEM algorithm with the default parameters. Average coverage was calculated for each contig by dividing the total number of bases mapped to the contig by the length of the contig. Relative abundance of a gene was determined by summing the average coverage of each contig that contained that gene and normalizing to the total mapped reads of that sample.

https://doi.org/10.1021/acs.est.3c07972
Environ. Sci. Technol. 2024, 58, 7056−7065

RESULTS

Impact of Groundwater Recharge on the Chemical and Isotopic Composition of Nitrogen Oxides at the FRC. The sampling of FRC groundwater from the SZ bracketed a dry period (August 29, 2019−October 16, 2019) followed by a two-week period of frequent rains that raised the water table (Figures 2 and S2). The rain-associated recharge

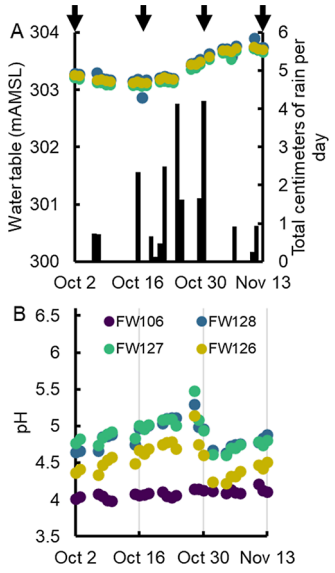

Figure 2. Impact of rain events on water table height (A) and pH (B) of selected wells. The months prior to sampling for isotopes (arrows, A) received less than 0.5 cm of rain per day. That dry period was followed by days of significant rain (bar plot, A) that restored the water table [colored filled circles, (A)] and coincided with a drop in pH [colored filled circles, (B)] for all but one well (FW106, purple).

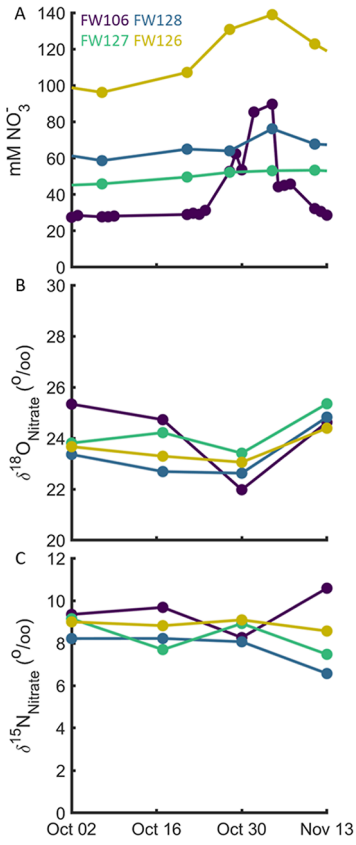

Figure 3. Nitrate concentration and isotopic composition were relatively constant throughout the time of sampling, indicating limited excursions in reaction or transport except for FW106. An increase in the nitrate concentration of water sampled from FW106 following rain (A) correlated with a shift to a lighter isotopic composition (B,C), suggesting a more variable influence of nitrate reduction on this water mass.

was correlated with an approximate 0.5 unit drop in pH for all wells except for FW106, which remained at pH 4. The dissolved oxygen was relatively constant at 0.2 ± 0.2 mg/L for most wells. Relatively invariant isotopic composition of the water ($\delta^{18}O$ and $\delta^{2}H$) during the observation period suggested that rain increased groundwater flow at the observed depths but did not alter its sources (Figure S3). However, isotopic composition did show that some nearby deep wells received water from at least two different sources, pointing to significant hydraulic heterogeneity, which was also reflected in changing nitrate concentrations over time. Groundwater nitrate originating from the former S3 waste disposal pond generally was within the range of 10−100 mM but reached 140 mM in some wells in the later part of the sampling period (October 30, 2019).

The isotopic composition of groundwater nitrate from the sampling wells was relatively constant but enriched in ^{15}N and ^{18}O relative to commonly reported values for synthetic nitrate (Figure S4), the expected source of nitrate in the S3 ponds. The relatively constant isotopic composition of nitrate throughout the observation period, despite excursions in concentration, suggested a combination of (1) an isotopically enriched source nitrate and (2) variable dilution and reduction of the primary source near the disposal pond before entering the groundwater or in transit to the sampled well (Figures 3 and S5). A notable exception was observed in groundwater from FW106, where the nitrate contributing to the increased well water concentration following the rain event exhibited markedly lower $\delta^{15}N$ and $\delta^{18}O$ values. Thus, there appear to be multiple sources of nitrate, some having experienced less denitrification and therefore maintaining proportionately lower $\delta^{15}N$ and $\delta^{18}O$ values.

The time-dependent nitrate concentrations and isotopic composition of groundwater in FW106 could also reflect the importance of reactive transport in the system. An increase in the subsurface flow rate following rain (Figure 2A) likely reduced the period of time nitrate was acted upon by microbial activity, retaining the lighter isotopic signature of the source. The isotopic shifts likely reflect primarily denitrification activity since more than 5 mM ammonia would be required for a measurable impact by nitrification or nitrifier-denitrification, a concentration greatly exceeding reported groundwater values of less than 0.5 mM (Figure S4).[32] Together, these observations reflect the complex hydrology contributing to different local nitrate sources in this highly altered system and highlight the need for improved reactive transport modeling of the site.

Sources and Sinks of Subsurface Nitrous Oxide. Nitrous oxide was quantified both in groundwater and as mass fluxes from separate wells screened at distinct depths. Here, we examine biotic and abiotic sources of production in groundwater through isotopic composition and activity measurements. We consider the gas flux data in relationship to possible nitrous oxide sinks in the following section.

https://doi.org/10.1021/acs.est.3c07972
Environ. Sci. Technol. 2024, 58, 7056−7065

Multiple processes, both biotic and abiotic, are known to contribute to nitrous oxide production. The primary contributing activities are denitrification by bacteria, archaea, and fungi, nitrification by bacteria and archaea, chemodenitrification, and dissimilatory nitrate reduction to ammonium by bacteria. The individual contributions to nitrous oxide production in an environmental system can be partially resolved by analyzing the natural isotopic composition of nitrous oxide. Analysis of the nitrous oxide site preference (SP) from multiple wells over a several weeks period (Figures 4 and S7) revealed both relatively stable (e.g., FW106, FW127, FW126, and FW103) and highly variable SP patterns (e.g., FW128, FW024, FW026, and FW104), with evidence for major contributions from both denitrification and chemodenitrification based on published meta-analyses of both pure culture and natural systems with defined or verified activity.[26]

The importance of chemodenitrification at this site is also supported by incubations with acetylene to block the NosZ activity. Active biological production and consumption of nitrous oxide was observed in groundwater sampled from GW271 in an area of low contamination, up gradient from the primary source of contamination, as shown by nitrous oxide accumulation only when acetylene was added to samples amended with organic carbon and nitrate. Addition of acetylene, organic carbon, and nitrate resulted in accumulation of significant nitrous oxide not observed with acetylene addition alone, indicative of the stimulation of a biotic source of nitrous oxide in areas of low carbon availability (Figure 5). In contrast, nitrous oxide production was observed for all treatments of highly contaminated groundwater sampled from FW106. The stimulation of production by addition of both carbon and acetylene is consistent with nitrous oxide primarily originating from an abiotic source and lesser from a biotic source. Nitrite was present at concentrations ranging from below detection (i.e., <0.5 μM) to 66 μM (mean = 7.8, median = 6.2) (Figure S6), consistent with it serving as a short-lived coreactant in chemodenitrification via iron oxidation as has been reported previously.[27] Although reduced iron or other natural reductants driving abiotic production have not been identified, the total iron concentration in groundwater is in the range of 60−180 g per kg of sediment and microbial reduction could provide a source of reduced iron.[32]

Biological consumption of nitrous oxide was suggested by the elevated δ^{18}O and δ^{15}N values of the nitrous oxide pool. Assuming the source was a combination of chemodenitrification and bacterial denitrification, as indicated by a mixing line between their previously reported values, enrichment in δ^{18}O and δ^{15}N of the nitrous oxide pool is likely due to a change in the source or an increase in contribution of nitrous oxide reduction (Figures 4 and S7).[26] The contribution of nitrous oxide reduction to isotopic enrichment was evident in several wells, as exemplified by well FW106. The decrease in the nitrous oxide concentration in groundwater received by this well on October 30, 2019 was correlated with strong increases in δ^{18}O and δ^{15}N values. The transient increase in nitrous oxide reduction activity appeared to be a system-level response to rainfall associated changes in pH and nitrate concentration (Figures 2, 3, S2, S5), and presumably other nutrients were flushed with this recharge event. However, the high variability in chemistry and biological response among wells colocalized by position and depth is additional evidence for subsurface hydraulic heterogeneity (Figures 4 and S7).

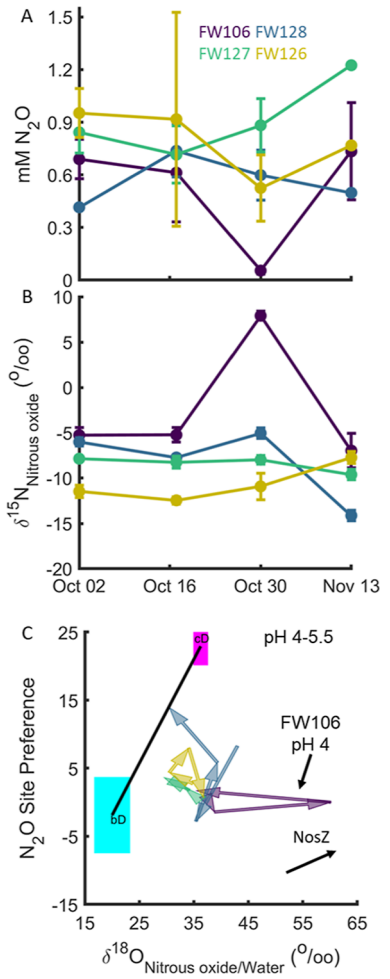

Figure 4. Temporal dynamics of nitrous oxide concentration (A) and isotopic composition (B) in the groundwater. Error bars show standard deviations of at most triplicate technical replicates. Active but variable biotic consumption of nitrous oxide is inferred from the increases in δ^{15}N (B) and δ^{18}O (C) associated with its reduction. Among wells and sampling periods, the most active reduction of source nitrous oxide was observed in well FW106 on October 30, as reflected by both the depletion of nitrous oxide and its corresponding enrichment in the heavier isotopes (B,C). The site preference (SP) of nitrous oxide and enrichment δ^{18}O values normalized by the $^{18}O/^{16}O$ of the accompanying groundwater (C) are consistent with both a mixed biotic-abiotic source of nitrous oxide and consumption through biotic reduction. Colored arrows denote the time course of compositional change of samples taken from each well as shown in panels (A,B). The black arrow indicates the temporal direction in SP and δ^{18}O composition when only biotic reduction acts on a sample. The solid black line connecting bacterial denitrification (bD, cyan box) and chemodenitrification (cD, magenta box) shows the expected variation in SP for a linear combination of both processes.[26] See Supporting Information Figure S7 for additional data.

Surface and Subsurface Flux of Nitrous Oxide. Nitrous oxide flux was measured at the surface and from wells screened at different depths to identify the regions of production and consumption (Figure 6). To correct for diffusion effects through the soil and sediment, the fluxes from wells were multiplied by the relative diffusion coefficient of a gas in homogeneous low porosity sand or clay (porosity = 0.2) compared to open air (D_{soil}/D_{air} = 0.03) (Figures 6 and S9, Supporting Information).[45] This diffusion model is supported by the flux response to rain events (Figure 6) where the

https://doi.org/10.1021/acs.est.3c07972
Environ. Sci. Technol. 2024, 58, 7056−7065

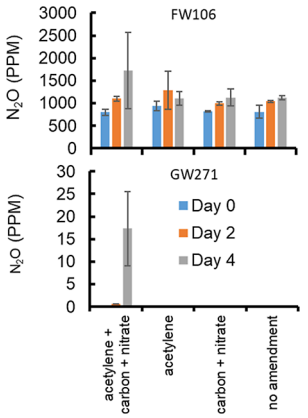

Figure 5. Acetylene block characterization of alternative nitrous oxide sources in FRC groundwater. A significant abiotic source of nitrous oxide in groundwater was supported by the addition of acetylene to block NosZ activity. Addition of acetylene to contaminated low pH groundwater sampled from FW106, with and without organic carbon supplementation, showed only a slight increase in production relative to that of unamended samples (upper panel). In contrast, all production in groundwater from a well (GW271) outside the contamination plume could be attributed to a biotic source when amended with organic carbon, nitrate, and acetylene (lower panel). Error bars represent the standard deviation of duplicate mesocosm experiments taken in November 2016 (FW106) and March 2017 (GW271).

increased sediment water content from rain restricted gas flow and increased well concentrations of nitrous oxide. The corrected fluxes were generally the highest near the variably SZ and decreased with proximity to the surface. Surface emissions were near the limit of detection and only somewhat higher near FW126, a location known to have higher permeability due to a gravel drainage channel (Supporting Information, Figure S9). The exception to this trend were higher fluxes measured from one shallow well (SG010). The proximity of SG010 to SG004, a well of much lower flux, suggests the higher flux in SG010 reflects either channeling due to subsurface heterogeneity or its localization in a hot spot of activity.

The general shape of the nitrous oxide flux profile suggests that nitrous oxide produced within the saturated and variably SZs is consumed by microbiota in the sediment column (VZ) before reaching the surface. In contrast, carbon dioxide flux, a more general measure of total heterotrophic microbial activity, increased from deeper depths to the near surface before decreasing at the surface. The lower surface flux likely reflects a normalization of flux as noted by the high temporal variability of well measurements (Figure S8) but steady emission from the surface, although autotrophic activity and carbon equilibration may be contributing factors (Figure 6).[46,47] These profiles both support a metabolically active VZ, potentially dominated by heterotrophic activity producing carbon dioxide and respiring available electron acceptors including nitrous oxide. However, an unusual feature of subsurface fluxes was high variability over a 24 h period, with the highest fluxes generally observed during the day (Figure S8). Published observations of similar diel variation in surface emissions from a variety of soil systems have been associated with diel variation in temperature.[48,49] Our observations of a diel cycling trend for nitrous oxide in an environment of near-constant temperature suggest a contribution of other factors and the sensitivity of this system to relatively minor shifts in

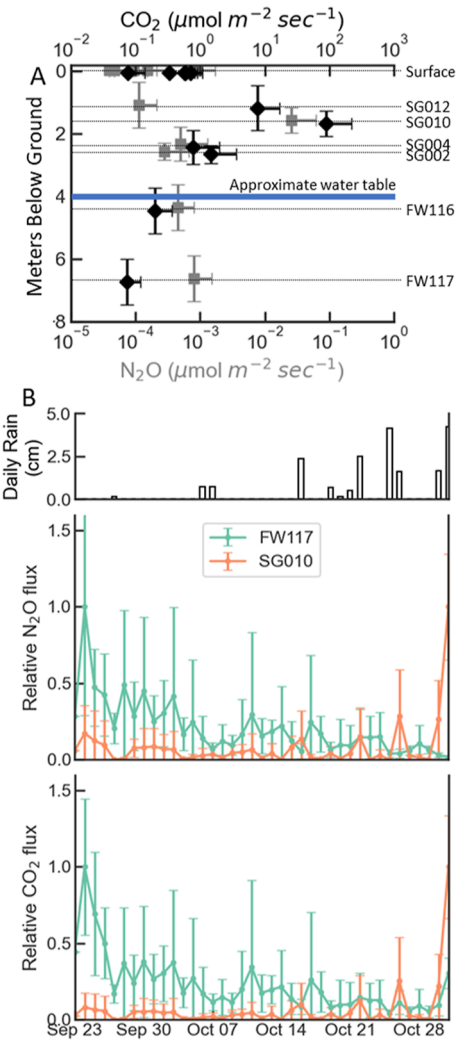

Figure 6. Nitrous oxide and carbon dioxide subsurface and surface flux. Nitrous oxide and carbon dioxide fluxes were determined from wells screened at different depths to estimate the flux of gas through the sediment column from September 22−27, 2019, representing at least 11 measurements for each location (A). Relative flux, as plotted, is the flux of a well normalized to the maximum observed for that well. All surface measurements are plotted to highlight their collectively negligible contributions. Two wells, FW117 and SG010, were monitored for an extended time to correlate well measurements with surface measurements taken October 7−9, 2019. The deeper well, FW117, was insensitive to rain events, while the shallower well, SG010, showed an increased flux on days with rain (B,C). Only FW117 and SG010 were monitored during the rain events.

water and nutrient movement, possibly related to surrounding land use.

Depth Resolved Mapping of the Genetic Potential for Nitrous Oxide Production and Consumption. A metagenomic analysis of soil cores collected from within and outside the contaminant plume was used to examine the depth-resolved relationship between the two *nosZ* variants and the nitrous oxide flux. The reductases were identified using co-occurrence of an ancillary gene (*nosR*). NosR is an FMN-binding flavoprotein present only in characterized Clade I organisms and implicated in electron transfer from the quinone pool to NosZ.[21] Since *nosR* is absent in Clade II organisms, the variants can be distinguished by the distribution of *nosZ* and *nosR*. Abundance of Clade I or II encoding populations was

https://doi.org/10.1021/acs.est.3c07972
Environ. Sci. Technol. 2024, 58, 7056−7065

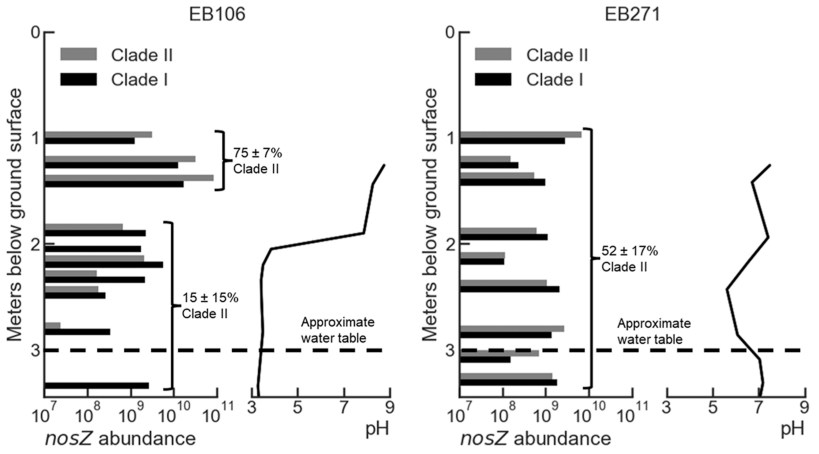

Figure 7. Depth distribution of *nosZ* variants within (EB106) and outside (EB271) the contaminant plume. The water table was approximately 3 m below the ground surface at the time of sampling.

determined by multiplying the abundance of *nosR* (Clade I) or *nosZ-nosR* (Clade II) relative to all genes in a sample, respectively, by the cells/gram of sediment at that location as measured previously.[32] This revealed a clear separation by depth in the core (EB106) collected from an area of high subsurface flux and low surface emissions (Figure 7). Clade II was the most abundant variant in the upper VZ, both numerically and as a fraction of all *nosZ*, whereas Clade I comprised a higher fraction of the two variants in the more acidic (pH ∼ 4) saturated region immediately above the water table. Thus, organisms expressing Clade II NosZ appear to be a major contributor to the consumption of nitrous oxide in this region of high subsurface nitrous oxide flux, functioning to largely suppress surface emissions of a potent greenhouse gas. This role of Clade II NosZ has also been proposed by others, based on observations in soil and the marine oxygen minimal zones.[23,24] In contrast to the core from within the contaminated zone, nitrous oxide off-gassing from all depths of the core (EB271) collected outside the contaminant plume was orders of magnitude lower than from EB106 immediately following coring.[32] Here, vertical stratification of Clade I and Clade II was less apparent with the two variants more equally distributed with depth.

Although our analysis clearly implicates Clade II in the suppression of nitrous oxide emissions, the physiological and environmental factors controlling the distribution and activity of organisms expressing either variant are very poorly constrained. Some available data point to a higher affinity for nitrous oxide and less inhibition by oxygen.[4,19,50] However, our data point to much more complex environmental controls of the distribution and activity. Also, since most of the Clade II containing organisms identified in our metagenomic survey are not represented in any of the major culture collections, a future emphasis on cultivation and isolation of environmentally relevant representatives will be key to constraining models to accurately predict net emission of nitrous oxide from the soil to the atmosphere.

Another physiologically and environmentally relevant feature of the denitrification pathway, based on complete genome sequence surveys, is the spotty organismal composition of genes in the canonical pathway. Complete pathway organisms appear to be relatively rare; most often, the pathway is interrupted or truncated. Some populations encode *nosZ* but lack other denitrification genes, known as nondenitrifying nitrous oxide reducers.[51] One consequence of fragmented pathway distribution is the organismal production of environmentally important intermediates (nitrite, nitric oxide, and nitrous oxide), suggesting their importance to combined biotic and abiotic activities and organismal partnering for achieving complete denitrification. The ecological significance of organismal partnering and environmental conditions conducive to partnering are mostly unrecognized and understudied areas of research.

The well-grounded dogma that "the environment selects" makes the Oak Ridge Field Research Center an important test bed for refining the understanding of the impact of gene variants, organism pathway composition and partnering, and environmental factors governing both biotic and abiotic nitrogen transformation and loss. The environment is not only selective (genotype) but also governs functional activity (phenotype). For example, even among organisms encoding the complete pathway, environmental factors such as pH, metal availability, and oxygen concentration influence the oxidation state of the final nitrogen product. Low pH, as is common at this field site, is well recognized to promote nitrous oxide production by inhibiting NosZ activity.[52] Yet the isotopic composition of nitrous oxide at the ORNL reservation clearly indicates NosZ activity at a pH of 4 (Figure 4). As a more complete collection of field relevant organisms is brought into culture for genetic and physiological characterization, those data will further inform field-based process observations. In turn, ongoing process-directed metagenomic, isotopic, chemical, and activity surveys will serve to identify locations within this contaminated field site for the hypothesis testing essential to developing more predictive models of reactive nitrogen transformation and flux.

■ ASSOCIATED CONTENT

Supporting Information

The Supporting Information is available free of charge at https://pubs.acs.org/doi/10.1021/acs.est.3c07972.

Additional data and figures about instrumentation, well characteristics, metagenome statistics, normalizations, and dynamics of other wells in the area are provided (PDF)

https://doi.org/10.1021/acs.est.3c07972
Environ. Sci. Technol. 2024, 58, 7056−7065

AUTHOR INFORMATION

Corresponding Author

Kristopher A. Hunt − *Department of Civil and Environmental Engineering, University of Washington, Seattle, Washington 98195, United States;* orcid.org/0000-0003-0024-4913; Phone: (206) 616-6985; Email: hunt0362@uw.edu

Authors

Alex V. Carr − *Department of Molecular Engineering Sciences, University of Washington, Seattle, Washington 98105, United States; Institute for Systems Biology, Seattle, Washington 98109, United States*

Anne E. Otwell − *Department of Civil and Environmental Engineering, University of Washington, Seattle, Washington 98195, United States*

Jacob J. Valenzuela − *Institute for Systems Biology, Seattle, Washington 98109, United States*

Kathleen S. Walker − *Biosciences Division, Oak Ridge National Laboratory, Oak Ridge, Tennessee 37830, United States; Department of Civil and Environmental Engineering, University of Tennessee, Knoxville, Tennessee 37996, United States*

Emma R. Dixon − *Biosciences Division, Oak Ridge National Laboratory, Oak Ridge, Tennessee 37830, United States; Department of Civil and Environmental Engineering, University of Tennessee, Knoxville, Tennessee 37996, United States*

Lauren M. Lui − *Environmental Genomics and Systems Biology, Lawrence Berkeley National Laboratory, Berkeley, California 94720, United States*

Torben N. Nielsen − *Environmental Genomics and Systems Biology, Lawrence Berkeley National Laboratory, Berkeley, California 94720, United States*

Samuel Bowman − *Department of Marine Chemistry and Geochemistry, Woods Hole Oceanographic Institution, Woods Hole, Massachusetts 02540, United States*

Frederick von Netzer − *Department of Civil and Environmental Engineering, University of Washington, Seattle, Washington 98195, United States*

Ji-Won Moon − *Biosciences Division, Oak Ridge National Laboratory, Oak Ridge, Tennessee 37830, United States*

Christopher W. Schadt − *Biosciences Division, Oak Ridge National Laboratory, Oak Ridge, Tennessee 37830, United States*

Miguel Rodriguez Jr − *Biosciences Division, Oak Ridge National Laboratory, Oak Ridge, Tennessee 37830, United States*

Kenneth Lowe − *Environmental Sciences Division, Oak Ridge National Laboratory, Oak Ridge, Tennessee 37830, United States*

Dominique Joyner − *Biosciences Division, Oak Ridge National Laboratory, Oak Ridge, Tennessee 37830, United States; Department of Civil and Environmental Engineering, University of Tennessee, Knoxville, Tennessee 37996, United States*

Katherine J. Davis − *Center for Biofilm Engineering, Montana State University, Bozeman, Montana 59717, United States;* orcid.org/0000-0002-0562-7035

Xiaoqin Wu − *Climate and Ecosystem Sciences Division, Lawrence Berkeley National Laboratory, Berkeley, California 94720, United States*

Romy Chakraborty − *Climate and Ecosystem Sciences Division, Lawrence Berkeley National Laboratory, Berkeley, California 94720, United States*

Matthew W. Fields − *Center for Biofilm Engineering and Department of Microbiology and Cell Biology, Montana State University, Bozeman, Montana 59717, United States*

Jizhong Zhou − *Climate and Ecosystem Sciences Division, Lawrence Berkeley National Laboratory, Berkeley, California 94720, United States; Institute for Environmental Genomics and Department of Botany and Microbiology, University of Oklahoma, Norman, Oklahoma 73019, United States; State Key Joint Laboratory of Environment Simulation and Pollution Control, School of Environment, Tsinghua University, Beijing 100084, China*

Terry C. Hazen − *Biosciences Division, Oak Ridge National Laboratory, Oak Ridge, Tennessee 37830, United States; Department of Civil and Environmental Engineering, University of Tennessee, Knoxville, Tennessee 37996, United States;* orcid.org/0000-0002-2536-9993

Adam P. Arkin − *Environmental Genomics and Systems Biology, Lawrence Berkeley National Laboratory, Berkeley, California 94720, United States; Department of Bioengineering, University of California Berkeley, Berkeley, California 94720, United States*

Scott D. Wankel − *Department of Marine Chemistry and Geochemistry, Woods Hole Oceanographic Institution, Woods Hole, Massachusetts 02540, United States;* orcid.org/0000-0002-7683-0225

Nitin S. Baliga − *Department of Molecular Engineering Sciences, University of Washington, Seattle, Washington 98105, United States; Institute for Systems Biology, Seattle, Washington 98109, United States*

David A. Stahl − *Department of Civil and Environmental Engineering, University of Washington, Seattle, Washington 98195, United States*

Complete contact information is available at: https://pubs.acs.org/10.1021/acs.est.3c07972

Notes

The authors declare no competing financial interest.

ACKNOWLEDGMENTS

This material by ENIGMA—Ecosystems and Networks Integrated with Genes and Molecular Assemblies (http://enigma.lbl.gov), a Science Focus Area Program at Lawrence Berkeley National Laboratory is based upon work supported by the U.S. Department of Energy, Office of Science, Office of Biological & Environmental Research under contract number DE-AC02-05CH11231.

REFERENCES

(1) Prather, M. J.; Hsu, J.; DeLuca, N. M.; Jackman, C. H.; Oman, L. D.; Douglass, A. R.; Fleming, E. L.; Strahan, S. E.; Steenrod, S. D.; Søvde, O. A.; Isaksen, I. S. A.; Froidevaux, L.; Funke, B. Measuring and Modeling the Lifetime of Nitrous Oxide Including Its Variability. *J. Geophys. Res.: Atmos.* **2015**, *120* (11), 5693−5705.

(2) Qi, C.; Zhou, Y.; Suenaga, T.; Oba, K.; Lu, J.; Wang, G.; Zhang, L.; Yoon, S.; Terada, A. Organic Carbon Determines Nitrous Oxide Consumption Activity of Clade I and II NosZ Bacteria: Genomic and Biokinetic Insights. *Water Res.* **2022**, *209*, 117910.

(3) Suenaga, T.; Riya, S.; Hosomi, M.; Terada, A. Biokinetic Characterization and Activities of N_2O-Reducing Bacteria in Response to Various Oxygen Levels. *Front. Microbiol.* **2018**, *9*, 697.

(4) Wang, Z.; Vishwanathan, N.; Kowaliczko, S.; Ishii, S. Clarifying Microbial Nitrous Oxide Reduction under Aerobic Conditions: Tolerant, Intolerant, and Sensitive. *Microbiol. Spectr.* **2023**, *11*, No. e04709.
(5) Braun, R. C.; Bremer, D. J. Nitrous Oxide Emissions in Turfgrass Systems: A Review. *Agron. J.* **2018**, *110* (6), 2222−2232.
(6) Panday, D.; Nkongolo, N. V. Soil Water Potential Control of the Relationship between Moisture and Greenhouse Gas Fluxes in Corn-Soybean Field. *Climate* **2015**, *3* (3), 689−696.
(7) Castaldi, S.; Bertolini, T.; Valente, A.; Chiti, T.; Valentini, R. Nitrous Oxide Emissions from Soil of an African Rain Forest in Ghana. *Biogeosciences* **2013**, *10* (6), 4179−4187.
(8) Dobbie, K. E.; Smith, K. A. Impact of Different Forms of N Fertilizer on N_2O Emissions from Intensive Grassland. *Nutr. Cycling Agroecosyst.* **2003**, *67* (1), 37−46.
(9) Aliyu, G.; Sanz-Cobena, A.; Müller, C.; Zaman, M.; Luo, J.; Liu, D.; Yuan, J.; Chen, Z.; Niu, Y.; Arowolo, A.; Ding, W. A Meta-Analysis of Soil Background N_2O Emissions from Croplands in China Shows Variation among Climatic Zones. *Agric., Ecosyst. Environ.* **2018**, *267*, 63−73.
(10) Sosulski, T.; Szara, E.; Szymańska, M.; Stępień, W.; Rutkowska, B.; Szulc, W. Soil N_2O Emissions under Conventional Tillage Conditions and from Forest Soil. *Soil Tillage Res.* **2019**, *190*, 86−91.
(11) Prosser, J. I.; Hink, L.; Gubry-Rangin, C.; Nicol, G. W. Nitrous Oxide Production by Ammonia Oxidizers: Physiological Diversity, Niche Differentiation and Potential Mitigation Strategies. *Global Change Biol.* **2020**, *26* (1), 103−118.
(12) Dore, J. E.; Popp, B. N.; Karl, D. M.; Sansone, F. J. A Large Source of Atmospheric Nitrous Oxide from Subtropical North Pacific Surface Waters. *Nature* **1998**, *396* (6706), 63−66.
(13) Arévalo-Martínez, D. L.; Kock, A.; Löscher, C. R.; Schmitz, R. A.; Bange, H. W. Massive Nitrous Oxide Emissions from the Tropical South Pacific Ocean. *Nat. Geosci.* **2015**, *8* (7), 530−533.
(14) Trimmer, M.; Chronopoulou, P. M.; Maanoja, S. T.; Upstill-Goddard, R. C.; Kitidis, V.; Purdy, K. J. Nitrous Oxide as a Function of Oxygen and Archaeal Gene Abundance in the North Pacific. *Nat. Commun.* **2016**, *7*, 13451−13510.
(15) Muñoz-Hincapié, M.; Morell, J. M.; Corredor, J. E. Increase of Nitrous Oxide Flux to the Atmosphere upon Nitrogen Addition to Red Mangroves Sediments. *Mar. Pollut. Bull.* **2002**, *44* (10), 992−996.
(16) Quick, A. M.; Reeder, W. J.; Farrell, T. B.; Tonina, D.; Feris, K. P.; Benner, S. G. Nitrous Oxide from Streams and Rivers: A Review of Primary Biogeochemical Pathways and Environmental Variables. *Earth Sci. Rev.* **2019**, *191* (February), 224−262.
(17) Hasegawa, K.; Hanaki, K.; Matsuo, T.; Hidaka, S. Nitrous Oxide from the Agricultural Water System Contaminated with High Nitrogen. *Chemosphere: Global Change Sci.* **2000**, *2* (3−4), 335−345.
(18) Yoon, S.; Nissen, S.; Park, D.; Sanford, R. A.; Löffler, F. E. Nitrous Oxide Reduction Kinetics Distinguish Bacteria Harboring Clade I NosZ from Those Harboring Clade II NosZ. *Appl. Environ. Microbiol.* **2016**, *82* (13), 3793−3800.
(19) Zhou, Y.; Suenaga, T.; Qi, C.; Riya, S.; Hosomi, M.; Terada, A. Temperature and Oxygen Level Determine N_2O Respiration Activities of Heterotrophic N_2O-reducing Bacteria: Biokinetic Study. *Biotechnol. Bioeng.* **2021**, *118* (3), 1330−1341.
(20) Conthe, M.; Wittorf, L.; Kuenen, J. G.; Kleerebezem, R.; Hallin, S.; van Loosdrecht, M. C. M. Growth Yield and Selection of *NosZ* Clade II Types in a Continuous Enrichment Culture of N_2O Respiring Bacteria. *Environ. Microbiol. Rep.* **2018**, *10* (3), 239−244.
(21) Hein, S.; Simon, J. Bacterial Nitrous Oxide Respiration: Electron Transport Chains and Copper Transfer Reactions; **2019**; pp 137−175. .
(22) Hallin, S.; Philippot, L.; Löffler, F. E.; Sanford, R. A.; Jones, C. M. Genomics and Ecology of Novel N_2O-Reducing Microorganisms. *Trends Microbiol.* **2018**, *26* (1), 43−55.
(23) Bertagnolli, A. D.; Konstantinidis, K. T.; Stewart, F. J. Non-denitrifier Nitrous Oxide Reductases Dominate Marine Biomes. *Environ. Microbiol. Rep.* **2020**, *12* (6), 681−692.
(24) Orellana, L. H.; Rodriguez-R, L. M.; Higgins, S.; Chee-Sanford, J. C.; Sanford, R. A.; Ritalahti, K. M.; Löffler, F. E.; Konstantinidis, K. T. Detecting Nitrous Oxide Reductase (*NosZ*) Genes in Soil Metagenomes: Method Development and Implications for the Nitrogen Cycle. *mBio* **2014**, *5* (3), 10.
(25) Lui, L. M.; Majumder, E. L.-W.; Smith, H. J.; Carlson, H. K.; von Netzer, F.; Fields, M. W.; Stahl, D. A.; Zhou, J.; Hazen, T. C.; Baliga, N. S.; Adams, P. D.; Arkin, A. P. Mechanism Across Scales: A Holistic Modeling Framework Integrating Laboratory and Field Studies for Microbial Ecology. *Front. Microbiol.* **2021**, *12*, 642422.
(26) Yu, L.; Harris, E.; Lewicka-Szczebak, D.; Barthel, M.; Blomberg, M. R. A.; Harris, S. J.; Johnson, M. S.; Lehmann, M. F.; Liisberg, J.; Müller, C.; Ostrom, N. E.; Six, J.; Toyoda, S.; Yoshida, N.; Mohn, J. What Can We Learn from N_2O Isotope Data? - Analytics, Processes and Modelling. *Rapid Commun. Mass Spectrom.* **2020**, *34* (20), No. e8858.
(27) Lim, N. Y. N.; Frostegård, Å.; Bakken, L. R. Nitrite Kinetics during Anoxia: The Role of Abiotic Reactions versus Microbial Reduction. *Soil Biol. Biochem.* **2018**, *119*, 203−209.
(28) Green, S. J.; Prakash, O.; Jasrotia, P.; Overholt, W. A.; Cardenas, E.; Hubbard, D.; Tiedje, J. M.; Watson, D. B.; Schadt, C. W.; Brooks, S. C.; Kostka, J. E. Denitrifying Bacteria from the Genus Rhodanobacter Dominate Bacterial Communities in the Highly Contaminated Subsurface of a Nuclear Legacy Waste Site. *Appl. Environ. Microbiol.* **2012**, *78* (4), 1039−1047.
(29) Peng, M.; Wang, D.; Lui, L. M.; Nielsen, T.; Tian, R.; Kempher, M. L.; Tao, X.; Pan, C.; Chakraborty, R.; Deutschbauer, A. M.; Thorgersen, M. P.; Adams, M. W. W.; Fields, M. W.; Hazen, T. C.; Arkin, A. P.; Zhou, A.; Zhou, J. Genomic Features and Pervasive Negative Selection in *Rhodanobacter* Strains Isolated from Nitrate and Heavy Metal Contaminated Aquifer. *Microbiol. Spectr.* **2022**, *10* (1), No. e02591.
(30) Van Den Heuvel, R. N.; Van Der Biezen, E.; Jetten, M. S. M.; Hefting, M. M.; Kartal, B. Denitrification at PH 4 by a Soil-Derived Rhodanobacter-Dominated Community. *Environ. Microbiol.* **2010**, *12* (12), 3264−3271.
(31) Smith, M. B.; Rocha, A. M.; Smillie, C. S.; Olesen, S. W.; Paradis, C.; Wu, L.; Campbell, J. H.; Fortney, J. L.; Mehlhorn, T. L.; Lowe, K. A.; Earles, J. E.; Phillips, J.; Techtmann, S. M.; Joyner, D. C.; Elias, D. A.; Bailey, K. L.; Hurt, R. A.; Preheim, S. P.; Sanders, M. C.; Yang, J.; Mueller, M. A.; Brooks, S.; Watson, D. B.; Zhang, P.; He, Z.; Dubinsky, E. A.; Adams, P. D.; Arkin, A. P.; Fields, M. W.; Zhou, J.; Alm, E. J.; Hazen, T. C. Natural Bacterial Communities Serve as Quantitative Geochemical Biosensors. *mBio* **2015**, *6*(3)..
(32) Moon, J.-W.; Paradis, C. J.; Joyner, D. C.; von Netzer, F.; Majumder, E. L.; Dixon, E. R.; Podar, M.; Ge, X.; Walian, P. J.; Smith, H. J.; Wu, X.; Zane, G. M.; Walker, K. F.; Thorgersen, M. P.; Poole II, F. L.; Lui, L. M.; Adams, B. G.; De León, K. B.; Brewer, S. S.; Williams, D. E.; Lowe, K. A.; Rodriguez, M.; Mehlhorn, T. L.; Pfiffner, S. M.; Chakraborty, R.; Arkin, A. P.; Wall, J. D.; Fields, M. W.; Adams, M. W.; Stahl, D. A.; Elias, D. A.; Hazen, T. C.; Hazen, T. C. Characterization of Subsurface Media from Locations Up- and down-Gradient of a Uranium-Contaminated Aquifer. *Chemosphere* **2020**, *255*, 126951.
(33) Christiansen, J. R.; Outhwaite, J.; Smukler, S. M. Comparison of CO_2, CH_4 and N_2O Soil-Atmosphere Exchange Measured in Static Chambers with Cavity Ring-down Spectroscopy and Gas Chromatography. *Agric. For. Meteorol.* **2015**, *211*−*212*, 48−57.
(34) Sigman, D. M.; Casciotti, K. L.; Andreani, M.; Barford, C.; Galanter, M.; Böhlke, J. K. A Bacterial Method for the Nitrogen Isotopic Analysis of Nitrate in Seawater and Freshwater. *Anal. Chem.* **2001**, *73* (17), 4145−4153.
(35) Casciotti, K. L.; Sigman, D. M.; Hastings, M. G.; Böhlke, J. K.; Hilkert, A. Measurement of the Oxygen Isotopic Composition of Nitrate in Seawater and Freshwater Using the Denitrifier Method. *Anal. Chem.* **2002**, *74* (19), 4905−4912.
(36) McIlvin, M. R.; Altabet, M. A. Chemical Conversion of Nitrate and Nitrite to Nitrous Oxide for Nitrogen and Oxygen Isotopic

https://doi.org/10.1021/acs.est.3c07972
Environ. Sci. Technol. 2024, 58, 7056−7065

Analysis in Freshwater and Seawater. *Anal. Chem.* **2005**, *77* (17), 5589−5595.
(37) Lui, L. M.; Nielsen, T. N.; Smith, H. J.; Chandonia, J.-M.; Kuehl, J.; Song, F.; Sczesnak, A.; Hendrickson, A.; Hazen, T.; Fields, M.; Arkin, A. P. *Sediment and Groundwater Metagenomes from Subsurface Microbial Communities from the Oak Ridge National Laboratory Field Research Center*; Res Sq: Oak Ridge, TN, USA, 2024, DOI: 10.21203/rs.3.rs-3401657/v1.
(38) Wu, X.; Gushgari-Doyle, S.; Lui, L. M.; Hendrickson, A. J.; Liu, Y.; Jagadamma, S.; Nielsen, T. N.; Justice, N. B.; Simmons, T.; Hess, N. J.; Joyner, D. C.; Hazen, T. C.; Arkin, A. P.; Chakraborty, R. Distinct Depth-Discrete Profiles of Microbial Communities and Geochemical Insights in the Subsurface Critical Zone. *Appl. Environ. Microbiol.* **2023**, *89* (6), No. e00500.
(39) Nurk, S.; Meleshko, D.; Korobeynikov, A.; Pevzner, P. A. MetaSPAdes: A New Versatile Metagenomic Assembler. *Genome Res.* **2017**, *27* (5), 824−834.
(40) Prjibelski, A.; Antipov, D.; Meleshko, D.; Lapidus, A.; Korobeynikov, A. Using SPAdes De Novo Assembler. *Curr. Protoc. Bioinf.* **2020**, *70* (1), No. e102.
(41) BBtools. 2016. BBTools. DOE Joint Genome Institute. https://jgi.doe.gov/data-and-tools/software-tools/bbtools/ (accessed Jul 25, 2023).
(42) Hyatt, D.; Chen, G.-L.; LoCascio, P. F.; Land, M. L.; Larimer, F. W.; Hauser, L. J. Prodigal: Prokaryotic Gene Recognition and Translation Initiation Site Identification. *BMC Bioinf.* **2010**, *11* (1), 119.
(43) Cantalapiedra, C. P.; Hernández-Plaza, A.; Letunic, I.; Bork, P.; Huerta-Cepas, J. EggNOG-Mapper v2: Functional Annotation, Orthology Assignments, and Domain Prediction at the Metagenomic Scale. *Mol. Biol. Evol.* **2021**, *38* (12), 5825−5829.
(44) Li, H.; Durbin, R. Fast and Accurate Short Read Alignment with Burrows-Wheeler Transform. *Bioinformatics* **2009**, *25* (14), 1754−1760.
(45) Stępniewski, W.; Sobczuk, H.; Widomski, M. Diffusion in Soils; **2011**; pp 214−220. .
(46) Baldocchi, D.; Chu, H.; Reichstein, M. Inter-Annual Variability of Net and Gross Ecosystem Carbon Fluxes: A Review. *Agric. For. Meteorol.* **2018**, *249*, 520−533.
(47) Hicks Pries, C. E.; Castanha, C.; Porras, R. C.; Torn, M. S. The Whole-Soil Carbon Flux in Response to Warming. *Science* **2017**, *355* (6332), 1420−1423.
(48) Wu, Y.; Whitaker, J.; Toet, S.; Bradley, A.; Davies, C. A.; McNamara, N. P. Diurnal Variability in Soil Nitrous Oxide Emissions Is a Widespread Phenomenon. *Global Change Biol.* **2021**, *27* (20), 4950−4966.
(49) Wu, S.; Chen, J.; Li, C.; Kong, D.; Yu, K.; Liu, S.; Zou, J. Diel and Seasonal Nitrous Oxide Fluxes Determined by Floating Chamber and Gas Transfer Equation Methods in Agricultural Irrigation Watersheds in Southeast China. *Environ. Monit. Assess.* **2018**, *190* (3), 122.
(50) Wittorf, L.; Bonilla-Rosso, G.; Jones, C. M.; Bäckman, O.; Hulth, S.; Hallin, S. Habitat Partitioning of Marine Benthic Denitrifier Communities in Response to Oxygen Availability. *Environ. Microbiol. Rep.* **2016**, *8* (4), 486−492.
(51) Sanford, R. A.; Wagner, D. D.; Wu, Q.; Chee-Sanford, J. C.; Thomas, S. H.; Cruz-García, C.; Rodríguez, G.; Massol-Deyá, A.; Krishnani, K. K.; Ritalahti, K. M.; Nissen, S.; Konstantinidis, K. T.; Löffler, F. E. Unexpected Nondenitrifier Nitrous Oxide Reductase Gene Diversity and Abundance in Soils. *Proc. Natl. Acad. Sci. U.S.A.* **2012**, *109* (48), 19709−19714.
(52) Hénault, C.; Bourennane, H.; Ayzac, A.; Ratié, C.; Saby, N. P. A.; Cohan, J.-P.; Eglin, T.; Gall, C. Le. Management of Soil PH Promotes Nitrous Oxide Reduction and Thus Mitigates Soil Emissions of This Greenhouse Gas. *Sci. Rep.* **2019**, *9* (1), 20182.

https://doi.org/10.1021/acs.est.3c07972
Environ. Sci. Technol. 2024, 58, 7056−7065